

# The Application of Molecular Mechanics to the Structures of Carbohydrates

G. A. Jeffrey and R. Taylor

Department of Crystallography, University of Pittsburgh, Pittsburgh, Pennsylvania 15260  
Received August 10, 1979

A study is reported of the accuracy with which the geometries of pyranose and methyl pyranoside molecules are predicted by molecular mechanics. Calculations of the conformational energies of the model compounds dihydroxymethane, methoxymethanol, and dimethoxymethane, made with the program MMI, produced results that compare well with previous *ab initio* molecular orbital calculations. This indicates that MMI gives a satisfactory account of the energetic and conformational aspects of the *anomeric effect*, a conclusion further supported by calculations on 2-methoxytetrahydropyran. The prediction of the observed preferred conformations of the primary alcohol group in aldohexopyranoses appears to be less satisfactory. MMI-CARB, a version of MMI with changes in some of the equilibrium C—O bond lengths of the program, has been used to calculate the geometries of 13 pyranose and methyl pyranoside molecules, the crystal structures of which have been studied by neutron diffraction. When the C—C—O—H torsion angles are constrained to approximately the values observed in the crystal structures, good agreement is obtained between the theoretical and experimental molecular geometries. The rms deviation for C—C and C—O bonds, excluding those significantly affected by thermal motion in the crystal structure determinations, is 0.005 Å. Corresponding figures for the valence angles that do not involve hydrogen atoms and for the ring torsion angles are 1.2° and 2.0°, respectively. The Cremer and Pople puckering parameters for the pyranose rings are reproduced within 0.026 Å in *Q* and 5.4° in  $\theta$ .

## INTRODUCTION

The application of the molecular mechanics program MMI<sup>1</sup> to a series of bridged ring 1,6-anhydropyranoses has already been shown<sup>2</sup> to yield predicted geometries in good agreement with those observed by crystal structure analysis. We now report an extension of these calculations to pyranose and methyl pyranoside molecules, which, in the absence of the anhydro bridged ring system, are believed to be more flexible and susceptible to crystal field distortions. For this reason the comparison provides a more rigorous test of how well molecular mechanics can reproduce the molecular geometry observed in the crystalline state for this type of molecule.

A major practical application of this approach lies in its extension to polysaccharides in which predictive model building is an essential component of fiber x-ray diffraction structure analysis. This extension, however, requires inclusion of intrasidue hydrogen bonding, which we have

avoided in this study by restricting our calculations to monosaccharides (the current version of MMI has no hydrogen bond potential).

## THE MOLECULAR MECHANICS CALCULATIONS

All calculations were done with MMI<sup>1</sup> on a DEC-1099 computer. Except when otherwise stated, the parameters used were those listed in the program documentation and reported by Allinger et al.<sup>3</sup> Oxygen lone pairs were treated as pseudoatoms with an equilibrium O—lone-pair distance of 0.5 Å and an equilibrium lone-pair—O—lone-pair angle of 140°.

The application of molecular mechanics to polar compounds such as carbohydrates is complicated by the necessity of estimating the energy due to electrostatic interactions between the dipoles as-

sociated with polar bonds.\* The two classical formulas commonly applied for this purpose are the Jeans formula for dipole-dipole interactions, used here, and the Coulomb formula for monopole-monopole interactions. Both are approximations based on the assumption that the distance between the interacting dipoles, or charges, is large compared with the extent of their distribution. In addition, it is difficult to define a suitable effective dielectric constant because the medium separating the interacting dipoles will not be uniform throughout the molecule. In this work we follow the practice of most workers by using values in the range 1-4.

The C—H, C—O, O—H, and O—lone-pair bond moments are those chosen by Allinger et al.<sup>3</sup> to reproduce the observed dipole moments of alcohols and ethers. It was uncertain how reliable these values are for carbohydrates, in which the inductive effect of the oxygen atoms may be expected to alter significantly the charge distribution around neighboring groups.<sup>†</sup>

### The Anomeric Effect<sup>‡</sup>

The anomeric carbon atom [C(1) in aldopyranoses] has unique chemical, conformational, and structural properties which arise from the fact that it is bonded to two oxygen atoms. *Ab initio* molecular orbital calculations suggest that the polarization of the C—O bonds causes a reduction in the  $\sigma$  electron density at the carbon atom, which is compensated for by a back donation of electron

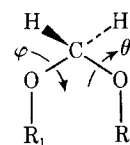
density from the oxygen lone pairs to the  $\sigma^*$  orbitals of adjacent bonds.<sup>8,9</sup> The extent to which this occurs depends on the degree of orbital overlap and therefore on the configuration at C(1) and the conformation about the anomeric [i.e., exocyclic C(1)—O] bond. Molecular orbital theory predicts that the maximum stabilization energy due to this effect is obtained when the anomeric group is axial rather than equatorial and the anomeric torsion angle [O(ring)—C(1)—O—H in aldopyranoses] is  $\pm 90^\circ$ .

In MMI this has been simulated by the introduction of a twofold torsional potential for the O—C—O—lone-pair sequence<sup>3</sup>:

$$E_{\text{O—C—O—LP}} = V_2(1 - \cos 2\theta)/2$$

where  $\theta$  is the lone-pair—O—C—O torsion angle. The value of  $V_2$ , which determines the calculated stabilization energy, was chosen with reference to only one experimental datum, that is,  $\Delta H^\circ$  for the axial to equatorial conversion of 2-methoxytetrahydropyran in tetralin solution.<sup>3</sup>

In the formalism of molecular mechanics the conformational energies of the anomeric linkage depend primarily on the balance between electrostatic, back-bonding, and van der Waals effects. To assess the reliability with which these factors are estimated by MMI we calculated the potential energies of dihydroxymethane (I), methoxymethanol (II), and dimethoxymethane (III) as a function of the R—O—C—O—R torsion angles.



I:  $R_1 = \text{H}, R_2 = \text{H}$

II:  $R_1 = \text{CH}_3, R_2 = \text{H}$

III:  $R_1 = \text{CH}_3, R_2 = \text{CH}_3$

\* The geometries of  $\alpha$ - and  $\beta$ -glucopyranose have been fairly well reproduced without explicit consideration of electrostatic interactions (see ref. 4). It is uncertain, however, whether such an approximation will be adequate when extended to, say, oligo- and polysaccharides. A close parallel is found in the conformational analysis of polypeptides, in which the importance of the dipole interactions between amide groups has long been recognized (see ref. 5).

<sup>†</sup> It has been noted<sup>6</sup> that even in simple compounds such as ethanol and 2-propanol the neglect of induced charges on carbon and  $\alpha$ -hydrogen atoms can lead to incorrect conformational predictions with MMI.

<sup>‡</sup> A general discussion of the anomeric and exoanomeric effects and references to the primary literature can be found in ref. 7.

These molecules have been investigated as model compounds for the anomeric effect in pyranoses and methyl pyranosides with *ab initio* molecular orbital (MO) methods. The results were in good agreement with the conformational properties and C—O bond length variations observed in the crystal structures of the pyranose and methyl pyranoside sugars.<sup>8,9</sup>

**Table I.** Calculated potential energy surfaces for dihydroxymethane.

$\varphi^a$	$\theta$						
	$-180^\circ$	$-120^\circ$	$-60^\circ$	$0^\circ$	$60^\circ$	$120^\circ$	$180^\circ$
$180^\circ$	7.1	6.1	3.4	3.4	3.4	6.1	7.1
	4.2	3.5	2.0	3.3	2.0	3.5	4.2
	(8.8)	(7.3)	(3.8)	(4.4)	(3.8)	(7.3)	(8.8)
$120^\circ$	6.1	6.0	3.6	2.8	2.2	5.0	6.1
	3.5	3.1	1.7	2.8	1.3	2.8	3.5
	(7.3)	(7.2)	(3.8)	(3.6)	(3.1)	(5.9)	(7.3)
$60^\circ$	3.4	3.6	3.9	3.4	0	2.2	3.4
	2.0	1.7	1.3	2.4	0	1.3	2.0
	(3.8)	(3.8)	(4.1)	(4.0)	(0)	(3.1)	(3.8)
$0^\circ$	3.4	2.8	3.4	8.2	3.4	2.8	3.4
	3.3	2.8	2.4	5.6	2.4	2.8	3.3
	(4.4)	(3.6)	(4.0)	(10.4)	(4.0)	(3.6)	(4.4)

<sup>a</sup> For each  $\varphi$  value the energies given in the first and second lines are those calculated with MMI, using dielectric constants of 1 and 3, respectively. The values in parentheses in the third line are taken from the *ab initio* MO results reported in ref. 9. A similar layout is used for Tables II–IV, except that no MO energies are given in Table IV. All energies are in kcal/mole.

In our calculations the bond lengths and valence angles were constrained to standard values (i.e., C—O, 1.43 Å; C—H, 1.09 Å; O—H, 0.96 Å; valence angles tetrahedral, methyl groups staggered in II and III), but the lone pairs were permitted to relax to their minimum-energy positions. The results, based on dielectric constant values of 1 and 3, are shown in Tables I—III with the comparable values from the *ab initio* MO calculations at the RHF/6-31G\* level for I and RHF/4-31G level for II and III. For all three compounds the MMI and HF MO calculations show the same general features in the potential energy surfaces. The agreement is particularly good for dihydroxymethane for which the more sophisticated RHF/6-31G\* basis set was used. Because earlier calculations on dihydroxymethane at the 4-31G level<sup>10</sup> showed greater separations between the various conformers than those subsequently calculated with the 6-31G\* basis set, it is reasonable to conclude that 6-31G\* calculations on II and III would also show results in closer correspondence with the MMI results.

The results in Tables II and III suggest that MMI overestimates the energies of conformations that involve close, nonbonded contacts between

**Table II.** Calculated potential energy surfaces for methoxymethanol.

$\varphi$	$\theta$						
	$-180^\circ$	$-120^\circ$	$-60^\circ$	$0^\circ$	$60^\circ$	$120^\circ$	$180^\circ$
$180^\circ$	5.3	4.5	2.1	2.6	2.1	4.5	5.3
	3.2	2.6	1.3	2.6	1.3	2.6	3.2
	(9.4)	(7.6)	(3.0)	(2.7)	(3.0)	(7.6)	(9.4)
$120^\circ$	7.3	7.0	4.8	4.7	4.0	6.4	7.3
	5.3	4.9	3.5	4.9	3.3	4.7	5.3
	(9.8)	(9.7)	(5.7)	(4.3)	(3.8)	(8.0)	(9.8)
$60^\circ$	2.3	3.0	5.7	5.6	0	1.3	2.3
	1.2	1.5	3.9	5.1	0	0.5	1.2
	(4.3)	(4.4)	(6.9)	(6.9)	(0)	(2.9)	(4.3)
$0^\circ$	5.1	7.8	11.4	42.8	11.4	7.8	5.1
	4.8	7.5	10.6	41.1	10.6	7.5	4.8
	(10.7)	(10.9)	(14.7)	(27.4)	(14.7)	(10.9)	(10.7)

**Table III.** Calculated potential energy surfaces for dimethoxymethane.

$\varphi$	$\theta$						
	$-180^\circ$	$-120^\circ$	$-60^\circ$	$0^\circ$	$60^\circ$	$120^\circ$	$180^\circ$
$180^\circ$	3.6	5.6	0.9	4.4	0.9	5.6	3.6
	2.1	4.1	0.2	4.2	0.2	4.1	2.1
	(7.7)	(8.1)	(2.6)	(9.0)	(2.6)	(8.1)	(7.7)
$120^\circ$	5.6	7.9	4.5	9.8	2.9	7.7	5.6
	4.1	6.3	3.5	9.7	2.3	6.4	4.1
	(8.1)	(10.4)	(5.6)	(11.5)	(3.3)	(8.5)	(8.1)
$60^\circ$	0.9	4.5	<sup>a</sup>	<sup>a</sup>	0	2.9	0.9
	0.2	3.5	<sup>a</sup>	<sup>a</sup>	0	2.3	0.2
	(2.6)	(5.6)	(18.9)	(18.7)	(0)	(3.3)	(2.6)
$0^\circ$	4.4	9.8	<sup>a</sup>	<sup>a</sup>	<sup>a</sup>	9.8	4.4
	4.2	9.7	<sup>a</sup>	<sup>a</sup>	<sup>a</sup>	9.7	4.2
	(9.0)	(11.5)	(18.7)	<sup>a</sup>	(18.7)	(11.5)	(9.0)

<sup>a</sup> Very large.

the methyl and hydroxyl hydrogen atoms. This indicates a deficiency in the empirical H...H van der Waals potential curves at short distances, which is of little importance, however, when the valence angles are allowed to change during energy minimization. This is borne out by the data in Table IV, which represent the MMI potential energy surfaces for dimethoxymethane with optimized bond lengths and valence angles.\*

\* This result supports the comments of Melberg and Rasmussen<sup>11</sup> on the errors arising from assuming rigid bond lengths and valence angles in conformational calculations on disaccharides.

**Table IV.** Calculated potential energy surfaces for dimethoxymethane (with optimized bond lengths and valence angles).

$\varphi$	$\theta$						
	$-180^\circ$	$-120^\circ$	$-60^\circ$	$0^\circ$	$60^\circ$	$120^\circ$	$180^\circ$
$180^\circ$	4.1	5.3	1.6	4.2	1.6	5.3	4.1
	2.5	3.8	0.9	4.1	0.9	3.8	2.5
$120^\circ$	5.3	6.7	3.4	6.3	2.8	6.6	5.3
	3.8	5.0	2.5	6.2	2.3	5.3	3.8
$60^\circ$	1.6	3.4	8.6	10.4	0	2.8	1.6
	0.9	2.5	7.7	10.0	0	2.3	0.9
$0^\circ$	4.2	6.3	10.4	21.2	10.4	6.3	4.2
	4.1	6.2	10.0	20.6	10.0	6.2	4.1

The potential energy surfaces calculated for dihydroxymethane show a marked dependence on the value chosen for the effective dielectric constant, but the importance of this parameter appears to diminish as the hydroxyls are replaced by methoxyls. Presumably this reflects the decreasing importance of electrostatic interactions in relation to van der Waals effects as the two hydroxyls are replaced by methoxyls. It seems likely that the calculated values of the glycosidic torsion angles in oligo- and polysaccharides will not be critically

dependent on the choice of effective dielectric constant.

### The Exoanomeric Effect

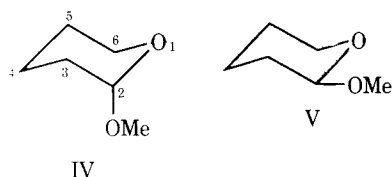
The anomeric torsion angles from the crystal structure analyses of 16 methyl pyranoside molecules (eight with axial anomeric groups and eight with equatorial) are listed with their means and standard deviations in Table V. These values are, of course, influenced by crystal field effects and do not necessarily reflect the conformational properties of isolated methyl pyranoside molecules. The consistency of the data, however, indicates that the equilibrium value of the anomeric torsion angle  $\varphi$  lies typically between  $60^\circ$  and  $70^\circ$  when the anomeric group is axial and between  $70^\circ$  and  $80^\circ$  when it is equatorial. This is consistent with the tenets of the *exoanomeric effect*.<sup>7</sup> The larger standard deviation of the equatorial pyranoside values implies that the potential energy necessary for small displacements of the methoxyl group from its equilibrium position is less when it is equatorial than when it is axial. Another feature commonly observed in the crystal structure anal-

**Table V.** Crystal structure torsion angles (deg) of methyl pyranosides.

	Anomeric torsion angle $\varphi$	Ring torsion angles			Cremer/ Pople ( $\theta$ )	Ref.
		C—C—O—C	C—C—C—O	C—C—C—C		
Axial anomeric group						
$\beta$ -L-arabino	68.9	61.8, -59.4	55.4, -58.2	55.5, -54.5	1.5	20
$\alpha$ -D-galacto	64.0	62.2, -58.4	52.4, -59.1	55.6, -52.3	4.9	18
$\alpha$ -D-gluco	62.7	58.4, -60.2	58.1, -54.6	53.9, -55.3	2.3	19
$\alpha$ -D-xylo (mol. 1)	70.5	60.8, -59.2	54.4, -55.2	50.2, -50.8	3.0	21
$\alpha$ -D-xylo (mol. 2)	62.5	60.0, -62.4	59.3, -54.0	51.4, -53.7	4.4	21
$\alpha$ -D-altro	64.1					22
$\alpha$ -D-manno	60.5					19
4-deoxy-4-fluoro $\alpha$ -D-gluco	66.2					23
mean of absolute values	65.0	60.3	56.1	53.3		
standard deviation	3.35					
Equatorial anomeric group						
$\alpha$ -L-arabino	-79.5	62.0, -59.9	55.8, -58.5	55.9, -55.2	1.5	20
$\beta$ -D-galacto	-77.1	65.3, -64.6	55.8, -57.7	52.1, -51.0	5.9	18
$\beta$ -D-gluco	-73.1	63.4, -67.9	61.5, -54.2	51.7, -54.3	7.0	24
$\beta$ -D-xylo	-72.1	63.1, -67.1	60.1, -53.1	49.1, -52.0	8.2	17
maltoside	-69.2					25
6-O-acetyl $\beta$ -D-gluco	-69.8					26
6-O-acetyl $\beta$ -D-galacto	-82.3					27
3,4-O-ethylidene $\beta$ -D-galacto	-69.7					28
mean of absolute values	74.1	64.2	57.1	52.7		
standard deviation	4.96					

ysis of pyranose molecules is illustrated by the ring torsion angles in Table V. The pyranosides with equatorial anomeric groups are more puckered than the corresponding axial pyranosides, due primarily to the larger C—C—O—C ring torsion angles.

We examined these effects to determine whether they would be reproduced by the molecular mechanics calculations; axial and equatorial 2-methoxytetrahydropyran (IV and V) were used:



The potential energy of these molecules was calculated as a function of the O—C—O—Me torsion angle. All other molecular parameters were allowed to relax during the energy-minimization procedure and an effective dielectric constant of 3 was used. The results are illustrated graphically in Figures 1 and 2. The torsional force constant for the O—C—O—Me group in each molecule was computed by a least-squares fit of calculated energies to the formula  $\Delta E = \frac{1}{2}k_\varphi\Delta\varphi^2$  ( $-10^\circ \leq \Delta\varphi \leq 10^\circ$ ). The results, together with the ring and anomeric torsion angles of the equilibrium conformations, appear in Table VI.

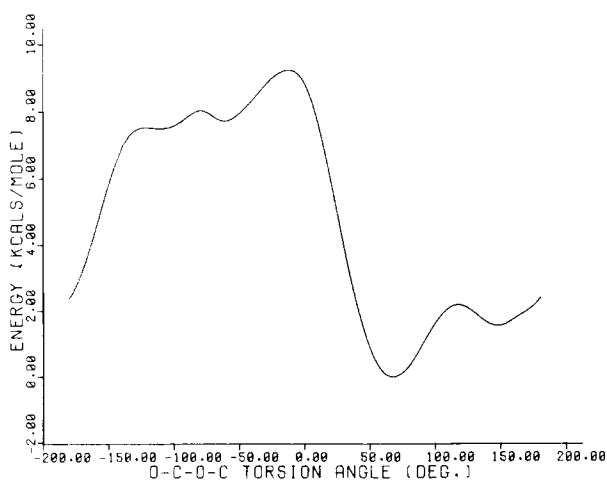


**Figure 1.** Torsional energy profile for axial 2-methoxytetrahydropyran.

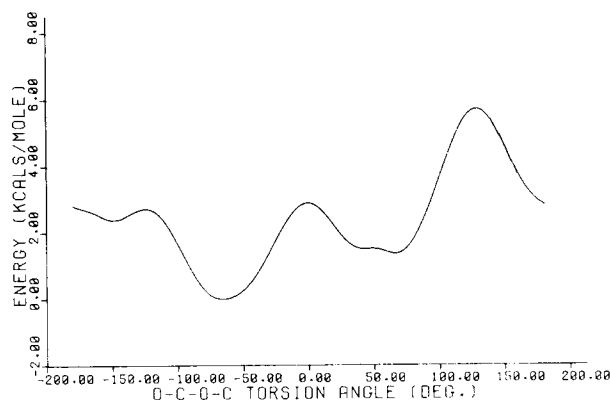


**Figure 2.** Torsional energy profile for equatorial 2-methoxytetrahydropyran.

**Table VI.** Calculated equilibrium geometries for axial and equatorial 2-methoxytetrahydropyran.

	Axial	Equatorial
Ring torsion angles ( $^\circ$ )		
C—C—O—C	60.1	62.1
	-59.8	-61.2
C—C—C—O	57.4	57.0
	-57.2	-57.6
C—C—C—C	53.8	52.5
	-54.3	-52.8
Cremer-Pople $\theta$ (deg)	0.0	1.7
Anomeric torsion angle (deg)	67.0	-64.0
Anomeric torsional force constant (mdyn Å/rad <sup>2</sup> )	0.115	0.044

The general features of the energy profiles are as expected. In the axial case the lowest minimum occurs at about  $+65^\circ$  and a second minimum, roughly 1.5 kcal/mole higher, at approximately  $+150^\circ$ . The broad maximum between  $0^\circ$  and  $-140^\circ$  is due primarily to steric interactions between the methyl group and the ring and ring substituent atoms. In the equatorial conformer there are three minima that correspond approximately to the three staggered arrangements about the anomeric bond with relative energies of ca. 0, 1.5, and 2.5 kcal/mole. The maximum near  $+130^\circ$  is due to interactions between the methyl group and the hydrogen atoms attached to C(3).

The calculated equilibrium values of the O—C—O—Me torsion angles do not reproduce the observation that  $\varphi(\text{equatorial}) > \varphi(\text{axial})$ . The difference is smaller and in the opposite sense. The torsional force constants, however, are consistent

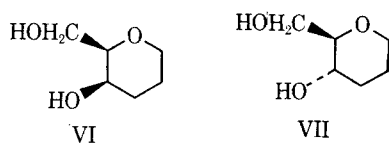
with the experimental data. The calculated ring puckering is greater for the equatorial conformer than for the axial, although the difference is not so great as that observed in the methyl pyranoside crystal structures.

Decreasing the effective dielectric constant to 1 has little effect on the results, the principal difference being a reduction in the anomeric torsion angles to  $-58.7^\circ$  for the equatorial conformer and  $+66.1^\circ$  for the axial conformer.

### The Primary Alcohol Group Conformation in Aldohexopyranoses

Another feature of interest in the aldohexopyranoses is the orientation of the primary alcohol group. An analysis of the available crystallographic data<sup>12</sup> shows that when the  $\text{—OH}$  group attached to the C(4) atom of the pyranose ring is equatorial the observed ratio of O(5)–C(5)–C(6)–O(6) conformers is 60% *gg* and 40% *gt*. When the  $\text{—O(4)H}$  group is axial, the ratio is 58% *gt* and 34% *tg*; the *gg* conformer has been observed twice but in each case was stabilized by intramolecular hydrogen bonding. These data can be rationalized in terms of the unfavorable "syn-diaxial" interactions between the  $\text{—O(4)H}$  and  $\text{—O(6)H}$  hydroxyl groups, which occur in the equatorial *tg* conformer and the axial *gg* conformer. In the free molecules and in solution an almost equal partition between the two more favorable conformations can be assumed.

The minimum energies of the *gg*, *gt*, and *tg* conformers of *cis*- and *trans*-2-hydroxymethyl-3-hydroxytetrahydropyran (VI and VII)



were computed to determine whether they were consistent with the above observations. With an effective dielectric constant of 3 the relative energies obtained for the *cis* isomer ( $\text{—CH}_2\text{OH}$  equatorial,  $\text{—OH}$  axial) were *gg*, +1.31, *tg*, +0.40, and *gt*, 0.00 kcal/mole. For the *trans* isomer

( $\text{—CH}_2\text{OH}$  equatorial,  $\text{—OH}$  equatorial) they were *tg*, +0.41, *gg*, +0.31, and *gt*, 0.00 kcal/mole. In both cases the conformer with the highest energy corresponds to the primary alcohol orientation which is not observed experimentally in the sugar molecules, but the energy differences are smaller than would be necessary to exclude the occurrence of the unfavorable orientation completely from the 71 crystal structures in which this observation is reported. In addition the movement of the hydroxyl groups away from the positions predicted by MMI affects the energies of the *gg*, *gt*, and *tg* conformers differently and therefore alters their relative energies. For both *cis* and *trans* isomers situations can arise in which the unfavorable conformer is not calculated to be the least stable. In the solid state, of course, the hydroxyl group orientations are determined largely by the crystal field environment.

The results were not significantly altered by changes in the effective dielectric constant. Neither do entropy effects appear to be important, for there is little difference between the conformers in the energy profiles for  $\pm 5^\circ$  displacements of the O—C—C—O torsion angles and their equilibrium values. We suspect that a modification to the hydrocarbon part of the force field is required to improve this comparison, but in view of the satisfactory performance of MMI in all other respects we did not pursue this question.\*

### Reproduction of the Anomeric Geometry in Pyranoses and Pyranosides

It is well known from crystal structure analyses that the C—O bond lengths and C—O—C and O—C—O valence angles of the anomeric moiety in pyranoses and pyranosides are influenced by the anomeric effect.<sup>14</sup> Because these features were not allowed for in the original parametrization of MMI, we have made appropriate changes in the equilibrium values for the bond lengths and va-

\* Allinger<sup>13</sup> has published preliminary details of a new force field, based on MMI but with a number of changes to the carbon and hydrogen parameters. It has been reported that these modifications solve some of the problems encountered<sup>3</sup> in the application of MMI to alcohols and ethers.

**Table VII.** Force field parameters for anomeric moiety.

<div style="display: flex; justify-content: space-around; align-items: center;"> <div style="text-align: center;"> <p>Axial</p> </div> <div style="text-align: center;"> <p>Equatorial</p> </div> </div>				
Bond stretching <sup>a</sup>	$r_0$ (Å)	$k_s$ (mdyn/Å)	$r_0$ (Å)	$k_s$ (mdyn/Å)
C(5)—O(5)	1.412	5.36	1.402	5.36
O(5)—C(1)	1.396	5.36	1.400	5.36
C(1)—O(1)	1.380	5.36	1.363	5.36
O(1)—C(H <sub>3</sub> )	1.388	5.36	1.388	5.36
Angle bending	$\theta_0$ (deg)	$k_\theta$ (mdyn Å/rad <sup>2</sup> )	$\theta_0$ (deg)	$k_\theta$ (mdyn Å/rad <sup>2</sup> )
C(5)—O(5)—C(1)	107.5	0.62	104.0	0.62
O(5)—C(1)—O(1)	109.3	0.56	104.9	0.56
C(1)—O(1)—C(H <sub>3</sub> )	105.3	0.62	105.3	0.62

<sup>a</sup> The equilibrium value for C—O bonds not associated with the anomeric group was changed to 1.405 Å, and that for O—H bonds to 0.970 Å.

lence angles associated with this group.\* The corresponding force constants have not been altered, for no reliable experimental information from which they could be derived is available. This is internally inconsistent, but unlikely to be a major source of error, because the energy terms involved are small compared with the total molecular steric energy.

Because the bonding situation depends on the stereochemistry at C(1), different parameters were needed for axial and equatorial anomeric groups; those chosen are listed in Table VII. To obtain better agreement between calculated geometries

\* This was done by redefining Allinger's atom types 8, 10, and 11 as ring oxygen, anomeric oxygen, and anomeric carbon atoms, respectively, and then specifying the required parameters in the manner described by the program documentation. The new equilibrium C—O bond lengths and C—O—C and O—C—O valence angles were chosen to obtain a reasonably good fit to the neutron diffraction geometries of three pyranosides. The use of as many as nine different standard C—O bond lengths may appear contrary to the general philosophy that molecular mechanics programs should reproduce experimental data with a minimum number of parameters. However, it illustrates that for highly polar compounds such as carbohydrates the bond stretching and valence angle deformation parameters are not always readily transferable. In the present case the C—O bonds in the anomeric sequence are strongly affected by their environment and cannot be treated as normal single bonds.

and those observed by neutron diffraction we also modified the equilibrium values of normal C—O and O—H bond lengths. This minor modification of the MMI parameters is referred to as MMI-CARB.

### Calculations of Pyranose and Methyl Pyranoside Geometries

MMI-CARB was used to calculate the geometries of 13 pyranoses and methyl pyranosides whose structures have been determined by neutron diffraction.<sup>15</sup> In preliminary calculations it was observed that the pyranose ring conformations are sensitive to changes in the C—C—O—H torsion angles. In the crystalline state the orientation of these hydroxyl groups is determined by hydrogen bonding, which is principally intermolecular. To make the experimental and calculated structures comparable we therefore constrained these angles to their approximate crystal structure values during energy minimization. This is equivalent to making some allowance for crystal field effects. Weak intramolecular hydrogen-bonding interactions occur in the crystal structures of  $\alpha$ -L-rhamnose,  $\beta$ -D-fructose, and  $\beta$ -L-lyxose, but they do not

**Table VIII.** Theoretical and experimental anomeric geometries.

	Number of observations	Theoretical mean	Experimental mean	Mean deviation <sup>a</sup>	rms deviation <sup>b</sup>
<b>Axial anomeric group</b>					
Bond lengths (Å)					
C(5)—O(5)	10	1.434	1.434	−0.001	0.006
O(5)—C(1)	10	1.415	1.419	−0.005	0.007
C(1)—O(1)	10	1.395	1.398	−0.003	0.007
O(1)—C(H <sub>3</sub> )	3	1.420	1.423	−0.003	0.003
Valence angles (°)					
C(5)—O(5)—C(1)	10	113.7	113.9	−0.2	0.5
O(5)—C(1)—O(1)	10	111.9	111.9	−0.1	1.0
C(1)—O(1)—C(H <sub>3</sub> )	3	113.5	113.8	−0.3	0.3
<b>Equatorial anomeric group</b>					
Bond lengths (Å)					
C(5)—O(5)	3	1.425	1.426	−0.001	0.005
O(5)—C(1)	3	1.419	1.428	−0.009	0.009
C(1)—O(1)	3	1.384	1.385	−0.001	0.006
O(1)—C(H <sub>3</sub> )	2	1.420	1.422	−0.002	0.005
Valence angles (°)					
C(5)—O(5)—C(1)	3	111.8	111.8	−0.1	1.1
O(5)—C(1)—O(1)	3	107.2	107.6	−0.5	0.9
C(1)—O(1)—C(H <sub>3</sub> )	2	113.8	113.1	0.7	0.7

<sup>a</sup> Mean deviation =  $\Sigma(x_{\text{theor}} - x_{\text{expt}})/N_{\text{obs}}$ .<sup>b</sup> rms deviation =  $[\Sigma(x_{\text{theor}} - x_{\text{expt}})^2/N_{\text{obs}}]^{1/2}$ .**Table IX.** Theoretical and experimental anomeric torsion angles.

	Theo- retical	Experi- mental
<b>Axial anomeric group</b>		
Methyl $\alpha$ -D-galactoside	65.7°	64.0°
Methyl $\alpha$ -D-glucoside	66.1	62.7
Methyl $\alpha$ -D-mannoside	65.8	60.5
<b>Equatorial anomeric group</b>		
Methyl $\beta$ -D-galactoside	−68.2	−77.1
Methyl $\beta$ -D-xyloside	−69.0	−72.1

appear to have a major influence on the molecular geometries. All calculations were done with an effective dielectric constant of 3. Calculations repeated with a lower value produced similar results, except that the agreement between the calculated and observed anomeric torsion angles was generally poorer.

The agreement between the experimental and theoretical anomeric geometries is summarized in Tables VIII and IX. The observed and calculated bond lengths and valence angles agree with rms deviations of 0.003–0.009 Å and 0.3°–1.1°, re-

spectively. The maximum discrepancy between observed and calculated anomeric torsion angles is 8.9° for methyl  $\beta$ -D-galactoside. Discrepancies of this magnitude could arise from crystal field effects because our calculations on equatorial 2-methoxytetrahydropyran indicate that only 0.2 kcal/mole is required to displace the torsion angle from its equilibrium value by  $\pm 10^\circ$ . Contrary to the result for 2-methoxytetrahydropyran, the absolute values of the anomeric torsion angles are now greater for equatorial anomeric than for axial groups, in accordance with the experimental observations.

Table X summarizes the results for the remaining bond lengths and angles (excluding the disordered  $-\text{CH}_2\text{OH}$  group in  $\alpha$ -L-sorbose). Apart from bonds associated with the primary alcohol groups, the experimental values of which we believe are significantly decreased by librational effects (the bond lengths for the crystal structures are not corrected for thermal motion), the rms deviation for C—C and C—O bonds is 0.005 Å. Bonds involving hydrogen atoms are less accurately reproduced but, again, this may be a libra-



**Table X.** Theoretical and experimental bond lengths and valence angles (excluding anomeric moieties and disordered  $\text{—CH}_2\text{OH}$  group in  $\alpha\text{-L-sorbose}$ ).

	Number of observations	Theoretical mean	Experimental mean	Mean deviation	rms deviation
Bond lengths (Å)					
C—C (ring)	52	1.527	1.526	0.001	0.005
C—C (exocyclic)	7	1.531	1.516	0.015	0.015
C—O (primary)	6	1.425	1.416	0.009	0.010
C—O (secondary)	39	1.419	1.420	−0.001	0.005
C—H	100	1.104	1.090	0.014	0.023
O—H	53	0.970	0.966	0.005	0.015
Valence angles (°)					
C—C—C (ring)	39	110.4	110.1	0.3	1.0
C—C—O (ring)	26	111.0	110.3	0.7	1.1
C—C—C (exocyclic)	7	112.9	112.5	0.5	1.1
C—C—O (exocyclic)	105	109.7	109.7	−0.1	1.3
C—C—H	130	109.9	109.1	0.8	1.8
O—C—H	108	107.7	109.2	−1.5	2.3
H—C—H	31	109.5	108.5	0.9	2.8
C—O—H	53	109.4	109.5	−0.2	2.3

tional phenomenon. The rms deviation for valence angles is about  $1.2^\circ$  when no hydrogen atoms are involved,  $2\text{--}3^\circ$  otherwise.

The experimentally observed trend for ring torsion angles ( $\text{CCOC} > \text{CCCO} > \text{CCCC}$ ) is reproduced as shown in Table XI. This is also a property of the unsubstituted tetrahydropyran ring (for which the calculated torsion angles are  $\text{CCOC} = 61.4^\circ$ ,  $\text{CCCO} = 57.8^\circ$ ,  $\text{CCCC} = 53.3^\circ$ ). The effect of this distortion is to decrease the  $\text{C—O—C}$  valence angle, which would otherwise be unfavorably large.\*

The Cremer–Pople puckering coordinates<sup>16</sup> of the theoretical and experimental structures are given in Table XII. The calculated rings tend to have lower  $Q$  values than the observed; that is, they are slightly less puckered. The  $\theta$  values agree reasonably well when the anomeric group is axial and the calculations reproduce the small difference

in the conformations of  $\beta\text{-L-arabinose}$  and  $\beta\text{-DL-arabinose}$  due, presumably, to the different crystal fields. This result is indicative of the magnitude of the dynamical changes in ring conformations that will occur in pyranose molecules in aqueous solution. The  $\theta$  values calculated for the pyranosides with equatorial anomeric groups are smaller than those observed, due primarily to an underestimation of the  $\text{CCOC}$  ring torsion angles. The large deviations between some of the theoretical and experimental  $\varphi_2$  values are of little significance because this parameter becomes indeterminate at  $\theta$  values near  $0^\circ$  or  $180^\circ$ .

## CONCLUSIONS

The present work on pyranoses and methyl pyranosides and that on the 1,6-anhydropyranoses<sup>2</sup> indicates that the molecular mechanics program MMI can be used with a significant degree of confidence to predict the molecular geometries of monosaccharides.

A satisfactory account of the *anomeric effect* provides configurational and conformational energy differences as good, if not better, than the state-of-the-art *ab initio* molecular orbital calculations.

\* Calculations on tetrahydropyran, with the ring torsion angles constrained to be equal to one another, indicate that this is the major factor causing the distortion. In pyranoses and pyranosides the energy gained by the reduction of the  $\text{C—O—C}$  valence angle is partly offset by an increase in the syn-diaxial repulsion between the substituents at C(1) and C(5). This interaction is likely to be of greater importance when the anomeric group is axial than when it is equatorial and may therefore explain the observation that the equatorial pyranosides are, in general, more puckered.

**Table XI.** Theoretical and experimental ring torsion angles (deg).

	Number of observations	Theoretical mean	Experimental mean	Mean deviation	rms deviation
Axial anomeric group					
C—C—O—C	20	59.1	59.5	−0.4	1.1
C—C—C—O	20	55.2	56.0	−0.8	1.6
C—C—C—C	20	52.7	54.3	−1.6	2.1
Equatorial anomeric group					
C—C—O—C	6	60.9	64.0	−3.1	3.8
C—C—C—O	6	56.5	56.5	0.0	2.5
C—C—C—C	6	52.2	51.5	0.7	1.7

**Table XII.** Theoretical and experimental Cremer–Pople puckering coordinates.

	Theoretical			Experimental		
	Q (Å)	$\theta$ (deg)	$\varphi_2$ (deg)	Q (Å)	$\theta$ (deg)	$\varphi_2$ (deg)
Axial anomeric group						
$\alpha$ -D-glucose	0.549	1.5	348.3	0.567	3.5	323.0
$\alpha$ -L-rhamnose	0.554	180.0	0.0	0.580	174.6	50.0
$\alpha$ -L-xylose	0.555	178.4	194.5	0.575	180.0	0.0
$\alpha$ -L-sorbose	0.547	180.0	0.0	0.553	178.3	219.9
$\beta$ -DL-arabinose <sup>a</sup>	0.563	2.2	99.4	0.584	2.1	139.5
$\beta$ -L-arabinose	0.561	1.3	82.8	0.573	1.5	116.3
$\beta$ -D-fructose	0.552	178.5	78.0	0.556	177.3	47.9
Methyl $\alpha$ -D-galactoside	0.562	3.6	293.0	0.570	4.9	276.4
Methyl $\alpha$ -D-glucoside	0.561	2.5	94.9	0.569	2.3	116.8
Methyl $\alpha$ -D-mannoside	0.558	2.5	81.9	0.556	0.0	0.0
Equatorial anomeric group						
$\beta$ -L-lyxose	0.563	177.3	211.2	0.570	177.1	187.0
Methyl $\beta$ -D-galactoside	0.575	3.7	278.8	0.582	5.9	346.7
Methyl $\beta$ -D-xyloside	0.559	3.9	355.3	0.580	8.2	36.4

<sup>a</sup> Figures given are for the L enantiomer.

The *exoanomeric effect* is also correctly predicted. It is surprising that the syn-diaxial interaction, which apparently excludes one of the three staggered orientations for the primary alcohol hydroxyl group in aldohexoses, is accounted for less satisfactorily.

Relatively minor changes were made to the equilibrium values of the bond lengths and some of the valence angles in the anomeric sequence to take into account the geometrical consequences of the anomeric effect. The calculated geometries of 13 pyranoses and methyl pyranosides gave excellent agreement with those measured experimentally by neutron diffraction crystal structure analyses. The agreement in bond lengths, valence, and ring torsion angles was of the order of 0.005 Å and 1° and 2°, respectively. Theoretical and ex-

perimental ring conformations agreed within 0.026 Å in Q and 5.4° in  $\theta$ .

This work was supported by Research Grant No. GM-24526 from the U.S. Public Health Service, National Institutes of Health.

## References

1. *Quantum Chemistry Program Exchange*, No. 318, Chemistry Department, Indiana University, Bloomington, IN.
2. G. A. Jeffrey and Y. J. Park, *Carbohydr. Res.*, **74**, 1 (1979).
3. N. L. Allinger and D. Y. Chung, *J. Am. Chem. Soc.*, **98**, 6798 (1976), and references therein.
4. K. Kildeby, S. Melberg, and K. Rasmussen, *Acta Chem. Scand. A*, **31**, 1 (1977).
5. D. A. Brant and P. J. Flory, *J. Am. Chem. Soc.*, **87**, 2791 (1965).
6. U. Burkert, *Tetrahedron*, **35**, 209 (1979).

7. E. L. Eliel, N. L. Allinger, S. J. Angyal, and G. A. Morrison, *Conformational Analysis*, Wiley-Interscience, New York, 1965, Chap. 6; J. F. Stoddart, *Stereochemistry of Carbohydrates*, Wiley-Interscience, New York, 1971, pp. 72–87.
8. G. A. Jeffrey, J. A. Pople, and L. Radom, *Carbohydr. Res.*, **38**, 81 (1974).
9. G. A. Jeffrey, J. A. Pople, J. S. Binkley, and S. Vishveshwara, *J. Am. Chem. Soc.*, **100**, 373 (1978).
10. G. A. Jeffrey, J. A. Pople, and L. Radom, *Carbohydr. Res.*, **25**, 117 (1972).
11. S. Melberg and K. Rasmussen, *Carbohydr. Res.*, **69**, 27 (1979).
12. S. Perez, J. St-Pierre, and R. H. Marchessault, *Can. J. Chem.*, **56**, 2866 (1978).
13. N. L. Allinger, *J. Am. Chem. Soc.*, **99**, 8127 (1977).
14. G. A. Jeffrey, in *Anomeric Effect, Origin and Consequences*, ACS Symp. Ser., W. A. Szarek and D. Horton, Eds., ACS, Washington, DC, 1979, Vol. 87, pp. 50–62.
15.  $\alpha$ -D-Glucose: G. M. Brown and H. A. Levy, *Science*, **147**, 1038 (1965).  $\alpha$ -L-Rhamnose: S. Takagi and G. A. Jeffrey, *Acta Crystallogr.*, **B34**, 2551 (1978).  $\alpha$ -L-Xylose: S. Takagi and G. A. Jeffrey, *Acta Crystallogr.*, **B35**, 1482 (1979).  $\alpha$ -L-Sorbose: S. Nordenson, S. Takagi, and G. A. Jeffrey, *Acta Crystallogr.*, **B35**, 1005 (1979).  $\beta$ -DL-Arabinose: S. Takagi, S. Nordenson, and G. A. Jeffrey, *Acta Crystallogr.*, **B35**, 991 (1979).  $\beta$ -L-Arabinose: ref. 17.  $\beta$ -D-Fructose: S. Takagi and G. A. Jeffrey, *Acta Crystallogr.*, **B33**, 3510 (1977). Methyl  $\alpha$ -D-galactoside: ref. 18. Methyl  $\alpha$ -D-glucoside: ref. 19. Methyl  $\alpha$ -D-mannoside: ref. 19.  $\beta$ -L-Lyxose: S. Nordenson, S. Takagi, and G. A. Jeffrey, *Acta Crystallogr.*, **B34**, 3809 (1978). Methyl  $\alpha$ -D-galactoside: ref. 18. Methyl  $\beta$ -D-xyloside: ref. 17.
16. D. Cremer and J. A. Pople, *J. Am. Chem. Soc.*, **97**, 1354 (1975).
17. S. Takagi and G. A. Jeffrey, *Acta Crystallogr.*, **B33**, 3033 (1977).
18. S. Takagi and G. A. Jeffrey, *Acta Crystallogr.*, **B35**, 902 (1979).
19. G. A. Jeffrey, R. K. McMullan, and S. Takagi, *Acta Crystallogr.*, **B33**, 728 (1977).
20. S. Takagi and G. A. Jeffrey, *Acta Crystallogr.*, **B34**, 1591 (1978).
21. S. Takagi and G. A. Jeffrey, *Acta Crystallogr.*, **B34**, 3104 (1978).
22. B. J. Poppleton, G. A. Jeffrey, and G. J. B. Williams, *Acta Crystallogr.*, **B31**, 2400 (1975).
23. W. Choong, N. C. Stephenson, and J. D. Stevens, *Cryst. Struct. Commun.*, **4**, 491 (1975).
24. G. A. Jeffrey and S. Takagi, *Acta Crystallogr.*, **B33**, 738 (1977).
25. S. S. C. Chu and G. A. Jeffrey, *Acta Crystallogr.*, **23**, 1038 (1967).
26. K. B. Lindberg, *Acta Crystallogr.*, **B32**, 642 (1976).
27. K. B. Lindberg, *Acta Crystallogr.*, **B32**, 645 (1976).
28. K. B. Lindberg, *Acta Crystallogr.*, **B32**, 639 (1976).